

1 **Sonogenetic modulation of cellular activities using an engineered auditory-sensing**
2 **protein**

3 Yao-Shen Huang^{1*}, Ching-Hsiang Fan^{2*}, Ning Hsu^{1*}, Chun-Yao Wu², Chu-Yuan Chang¹, Shi-
4 Rong Hong¹, Ya-Chu Chang¹, Anthony Yan-Tang Wu^{3,4,5}, Vanessa Guo³, Yueh-Chen Chiang¹,
5 Wei-Chia Hsu¹, Nai-Hua Chiu², Linyi Chen^{1,6}, Charles Pin-Kuang Lai^{3,4,7}, Chih-Kuang Yeh²,
6 Yu-Chun Lin^{1,6}

7

8 ¹Institute of Molecular Medicine, National Tsing Hua University, Hsinchu, 300, Taiwan

9 ²Department of Biomedical Engineering and Environmental Sciences, National Tsing Hua
10 University, Hsinchu, 300, Taiwan

11 ³Institute of Atomic and Molecular Sciences, Academia Sinica, Taipei, 106, Taiwan

12 ⁴Chemical Biology and Molecular Biophysics Program, Taiwan International Graduate
13 Program, Academia Sinica, Taipei, 106, Taiwan

14 ⁵Department and Graduate Institute of Pharmacology, National Taiwan University, 106,
15 Taiwan

16 ⁶Department of Medical Science, National Tsing Hua University, Hsinchu, 300, Taiwan

17 ⁷Genome and Systems Biology Degree Program, National Taiwan University and Academia
18 Sinica, Taipei, 106, Taiwan.

19

20 *These authors contributed equally to this work

21 Correspondence and requests for materials should be addressed to ckyeh@mx.nthu.edu.tw

22 and ycl@life.nthu.edu.tw

23

24
25
26
27
28
29
30
31
32
33
34
35
36
37
38
39
40
41
42
43
44
45
46

Abstract

Biomolecules that respond to different external stimuli enable the remote control of genetically modified cells. Chemogenetics and optogenetics, two tools that can control cellular activities via synthetic chemicals or photons, respectively, have been widely used to elucidate underlying physiological processes. These methods are, however, very invasive, have poor penetrability, or low spatiotemporal precision, attributes that hinder their use in therapeutic applications. We report herein a sonogenetic approach that can manipulate target cell activities by focused ultrasound stimulation. This system requires an ultrasound-responsive protein derived from an engineered auditory-sensing protein prestin. Heterogeneous expression of mouse prestin containing two parallel amino acid substitutions, N7T and N308S, that frequently exist in prestins from echolocating species endowed transfected mammalian cells with the ability to sense ultrasound. An ultrasound pulse of low frequency and low pressure efficiently evoked cellular calcium responses after transfecting with prestin(N7T, N308S). Moreover, pulsed ultrasound can also non-invasively stimulate target neurons expressing prestin(N7T, N308S) in deep regions of mice brains. Our study delineates how an engineered auditory-sensing protein can cause mammalian cells to sense ultrasound stimulation. Moreover, owing to the great penetration of low-frequency ultrasound (~400 mm in depth), our sonogenetic tools will serve as new strategies for non-invasive therapy in deep tissues of large animals like primates.

47

Introduction

48

49

50

51

52

53

54

55

56

Approaches that can non-invasively stimulate target cells buried in the deep tissues are highly desirable for basic research and clinical therapy. Currently, different external stimuli including photons, chemicals, radio waves, and magnetic fields have been used to stimulate target cells implanted with stimulus-responsive proteins or nanoparticles¹⁻⁴. However, these strategies suffer from several drawbacks including invasiveness, poor spatiotemporal precision, or low penetration depth, which greatly hinder their potential use in clinical therapy. To overcome these long-standing problems, we aim to use focused ultrasound (FUS) as a stimulus to remotely control cellular activities because it can non-invasively deliver acoustic energy to deep tissues while retaining spatiotemporal coherence⁵.

57

58

59

60

61

62

63

64

65

66

67

68

69

Ultrasound waves have frequencies greater than those of sound waves that can be heard by humans (>20 kHz). Low-frequency ultrasound waves (<3.5 MHz) are easily transmitted through tissues, including those of bones and brains⁶. Owing to its deep penetrability and spatiotemporal resolution (a few cubic millimetres), ultrasound-based neuromodulation has been tested on cultured neuronal cells and in brains of various model organisms⁶⁻¹¹. As continuous ultrasound waves or pulsed ultrasound waves of high acoustic pressure are typically needed to activate neurons, neuronal cells are likely to be weakly sensitive to ultrasound stimulus^{8,12,13}. To overcome this, gas-filled microbubbles (MBs) that vibrate upon ultrasound excitation have been used as ultrasound amplifiers to enhance their mechanical effects on target cells^{14,15}. Recently, Ibsen and colleagues used MBs to transduce mechanical stimulation from ultrasound waves to neuronal cells in *Caenorhabditis elegans* and induced behavioural output¹⁶. The pore-forming cationic mechanotransduction ion channel TRP-4 may be involved in transducing ultrasound stimulation onto MBs attached to *C. elegans*¹⁶. Although this study

70 verified that ultrasound-mediated neuromodulation is possible, its further development faces
71 major roadblocks, i.e., MBs have a short lifespan *in vivo* (<5 min in the blood), and it is
72 difficult to deliver MBs to extravascular tissues¹⁷. Compared with MBs, gas-filled protein
73 complexes, denoted as gas vesicles, are highly stable both *in vitro* and *in vivo* and efficiently
74 oscillate in response to ultrasound excitation. Different gas vesicle variants can serve as
75 genetically encoded ultrasound contrast reagents to track target microbes or cells by ultrasound
76 imaging^{18,19}. However, it is still challenging to express and assemble prokaryotic gas vesicles
77 in mammalian cells⁵. Recently, several groups implanted mechanosensitive ion channels, such
78 as Msc1 and Piezo1, into *in vitro* cell culture systems and, with their use, successfully perturbed
79 the cellular membrane potentials of target cells using ultrasound.^{20,21} However, the ultrasound
80 frequencies used in those studies are too high (30 MHz and 43 MHz) to be applicable for *in*
81 *vivo* use owing to their low penetrability (<5 mm). Therefore, to date, there has been no
82 sonogenetic system that uses low-frequency and low-pressure ultrasound to remotely control
83 activities of mammalian cells that have been genetically modified.

84 Several mammalian species, including bats and cetaceans, use ultrasound to navigate
85 or communicate. The high-frequency auditory sensitivity and selectivity in echolocating
86 mammals have been attributed to adaptive mechanical amplification in the outer hair cells
87 (OHCs) of their cochlea²². Prestin (also known as SCL26A5) is a transmembrane protein
88 residing in OHCs that drives their electromotility and seems to be involved in the ability to
89 hear ultrasound^{23–25}. Heterologous expression of prestin endows transfected mammalian cell
90 lines with several of the physiological hallmarks of OHCs, suggesting that prestin may
91 inherently act as an electromechanical transducer²⁶. Evolutionary analysis also suggests that
92 prestin is involved in ultrasound sensing of echolocating mammals²³. The primary sequence of

93 prestin is largely conserved among various mammalian species, although several specific
94 amino acid substitutions that directly affect the electromotility capacity of prestin frequently
95 occur in prestins of sonar mammals but not in those of their non-sonar counterparts^{23,24}. Thus
96 prestin probably enhances ultrasound sensitivity in mammals, although how it does so is still
97 unclear.

98

99

Results and discussion

100 Here we first examined the amino acid sequences of prestin from six non-echolocating
101 species and eight echolocating species. Asn at positions 7 and 308 in prestins of non-
102 echolocating species is frequently replaced with Thr and Ser, respectively, in echolocating
103 species (Fig. 1a). To test whether these apparently evolutionarily driven amino acid
104 substitutions are important to adaptive ultrasound sensing, two mutations N7T and/or N308S
105 were introduced into mouse prestin (hereafter mPrestin). The constructs used for our study
106 were wild-type prestin (mPrestinWT); mPrestin mutants containing a single substitution,
107 mPrestin(N7T) and mPrestin(N308S); and a mutant containing two substitutions,
108 mPrestin(N7T, N308S). Each of these constructs was tagged with the yellow fluorescent
109 protein Venus. Each construct was co-transfected with the calcium biosensor cyan fluorescence
110 protein (CFP)-R-GECO into the human HEK293T cell line. The calcium influx of transfected
111 cells was used as a readout in response to the mechanical stimulation of ultrasound wave. To
112 simultaneously excite FUS and acquire real-time cell images, an ultrasound transducer
113 connected to a waveform generator and an amplifier was placed on top of the live-cell imaging
114 system. This system focuses ultrasound waves to a circle with a diameter of a few millimetres
115 over a monolayer of cultured cells (Extended Data Fig. 1). Using this ultrasound-imaging

116 system, we stimulated cells co-expressing CFP-R-GECO and Venus-mPrestin(N7T, N308S) or
117 co-expressing CFP-RGECO and Venus with a short, low-frequency ultrasound pulse (0.5 MHz,
118 all pulses consisted of 3-sec duration, 2000 cycles, 10 Hz, 0.5 MPa unless otherwise noted).
119 Live-cell imaging showed that a short ultrasound pulse of 0.5 MHz was sufficient to evoke
120 calcium influx in cells expressing Venus-mPrestin(N7T, N308S), but not in cells transfected
121 with Venus alone (Fig. 1b; Extended Data Video 1). Quantification of the calcium imaging data
122 indicated that FUS induced a $351 \pm 20\%$ (mean \pm s.e.m.) increase in the R-GECO fluorescence
123 of Venus-mPrestin(N7T, N308S)-transfected cells (Fig. 1c, right panel). However, FUS only
124 slightly evoked the calcium response in cells that expressed Venus-mPrestinWT (Fig. 1c,
125 middle panel). Cells transfected with Venus alone did not respond to FUS stimulation (Fig. 1c,
126 left panel). These results indicated that heterogeneous expression of Venus-mPrestinWT
127 endowed the transfected cells with a weak ability to sense ultrasound. Substituting Thr at
128 position 7 and Ser at position 308 in the Venus-tagged mPrestinWT substantially improved the
129 ultrasound-evoked calcium response of the transfected HEK293T cells.

130 To determine the optimal ultrasound frequency/frequencies for cell manipulation, we
131 next comprehensively tested the calcium responses of cells expressing the various Venus-
132 mPrestin constructs to different FUS frequencies between 80 kHz and 3.5 MHz (3-sec duration,
133 2000 cycles, 0.5 MPa; Fig. 2). Interestingly, cells individually expressing the WT and mutated
134 constructs were sensitive only to 0.5 MHz FUS (Fig. 2). The 80 kHz, 1 MHz, 2 MHz, and 3.5
135 MHz FUS were insufficient to evoke a calcium influx in the cells (Fig. 2). Upon stimulation
136 by 0.5 MHz FUS, the percentage of ultrasound-responsive cells was 11.29 ± 4.25 -fold (mean
137 \pm s.e.m.) greater for the Venus-mPrestin(N7T, N308S) group compared with the control group
138 ($p = 0.024$; Fig. 2). Heterogeneous expression of Venus-mPrestinWT, Venus-mPrestin(N7T),

139 and Venus-mPrestin(N308S) only slightly increased the sensitivity of the transfected HEK293T
140 cells to 0.5 MHz FUS ($p = 0.31, 0.51, \text{ and } 0.25$, respectively; Fig. 2). These results confirmed
141 that 0.5 MHz FUS efficiently evoked a calcium response in cells expressing mPrestin(N7T,
142 N308S) in a frequency-dependent manner.

143 In addition to prestin, Ibsen and colleagues demonstrated that the mechanosensitive ion
144 channel, TRP-4, is required for ultrasound-mediated mechanical stimulation and can modify
145 animal behaviour in the presence of MBs¹⁶. To test whether TRP-4 can act as an ultrasound-
146 responsive protein, we transfected HEK293T cells with two members of the mammalian
147 TRPC4 family including human TRPC4 α (hTRPC4 α) and mouse TRPC4 β (mTRPC4 β)^{27,28}.
148 The calcium response of cells expressing hTRPC4 α or mTRPC4 β tagged with CFP upon FUS
149 stimulation of different frequencies was examined and quantified. The percentage of
150 ultrasound-excitable cells in the in the mTRPC4 β -CFP group was 3.29 ± 0.94 -fold (mean \pm
151 s.e.m.) greater than the control group upon stimulation with 0.5 MHz FUS ($p = 0.044$;
152 Extended Data Fig. 2). Ultrasound of 80 kHz, 1 MHz, 2 MHz, and 3.5 MHz was not sufficient
153 to induce a calcium response in cells expressing mTRPC4 β -CFP. Thus, mTRPC4 β -CFP is
154 only weakly sensitive to 0.5 MHz FUS. Although its protein sequence is very similar to
155 that of mTRPC4 β , hTRPC4 α -CFP did not respond to the low-frequency ultrasound
156 stimulation at all (Extended Data Fig. 2). Taken together, the comprehensive examination
157 of ultrasound sensing in cells transfected with different putative ultrasound-responsive
158 proteins shows that mPrestin(N7T, N308S) was the most responsive protein.

159 We next explored the possible molecular mechanisms that make the two
160 evolutionarily conserved amino acid substitutions important for prestin-dependent
161 ultrasound sensing. Targeting of prestin to the plasma membrane is required for its

162 function²⁹. Confocal images of Venus-mPrestinWT and Venus-mPrestin(N7T, N308S) in
163 living cells showed that Venus-mPrestinWT localised to the cytosol and to the plasma
164 membrane, whereas Venus-mPrestin(N7T, N308S) localised exclusively to the plasma
165 membrane (Fig. 3a). Quantification of the relative intensities confirmed that
166 mPrestin(N7T, N308S) exhibited a significantly greater plasma membrane/cytosol
167 intensity ratio than did Venus-mPrestinWT ($p = 0.003$; Fig. 3b). We therefore
168 hypothesised that targeting mPrestin(N7T, N308S) to the plasma membrane is important
169 for its sensitivity to ultrasound. To assess this hypothesis, we introduced a point mutation
170 (Y667Q) that causes prestin to mislocate to the Golgi apparatus into Venus-
171 mPrestin(N7T, N308S). As expected, Venus-mPrestin(N7T, N308S, Y667Q) accumulated
172 at the Golgi apparatus, and its plasma membrane/cytosol intensity ratio decreased
173 significantly ($p = 1.02E-7$; Fig. 3a, b). The mislocalisation of Venus-mPrestin(N7T, N308S,
174 Y667Q) to the Golgi apparatus impaired its ultrasound-sensing ability ($p = 0.032$; Fig. 3c),
175 confirming that plasma-membrane targeting of Venus-mPrestin(N7T, N308S) is required
176 for its response to ultrasound.

177 Venus-mPrestin(N7T, N308S) was not evenly distributed in the plasma membrane
178 but was concentrated in punctate regions (Figs. 1b and 3a). HEK293T cells expressing
179 mPrestin(N7T, N308S) exhibit significantly higher number of puncta than cells
180 expressing wild-type mPrestin ($p=0.015$; Extended Data Fig. 3a). Mislocation of
181 mPrestin(N7T, N308S, Y667Q) at Golgi reduces the number of puncta suggesting puncta
182 formation of mPrestin requires its plasma membrane targeting ($p=0.032$; Extended Data
183 Fig. 3a). Quantification data show the area of mPrestin(N7T, N308S) puncta is 132 ± 6.28
184 nm^2 (mean \pm s.e.m.; Extended Data Fig. 3b). Prestin self-assembles into oligomers to form

185 bullet-shaped complexes in the plasma membrane^{30,31}. To evaluate whether self-
186 association of prestin occurred in these punctate regions, we used fluorescence
187 resonance energy transfer (FRET) to examine the oligomerisation of Venus- and CFP-
188 tagged mPrestin constructs. A greater FRET efficiency was obtained in the punctate
189 regions of cells expressing mPrestin(N7T, N308S) as compared with cells transfected
190 with mPrestinWT ($p = 0.025$; Extended Data Fig. 3c, d), indicating that self-association of
191 mPrestin(N7T, N308S) but not mPrestinWT occurred in the punctate regions.
192 Immunofluorescence staining also showed that mPrestin(N7T, N308S) puncta associated
193 with actin filaments and microtubules (Extended Data Fig. 3e). Next, ultrafast imaging of
194 cells transfected with Venus-mPrestin(N7T, N308S) (imaging interval, 17 ms) was used
195 to observe the real-time behaviour of Venus-mPrestin(N7T, N308S) puncta upon FUS
196 stimulation. Live-cell imaging and quantification showed that Venus-mPrestin(N7T,
197 N308S) puncta oscillated continuously for a few seconds after being exposed to pulsed
198 0.5 MHz FUS (Fig. 3d, e; Extended Data Video 2). Because several waves of calcium
199 responses were observed after a single FUS pulse in the Venus-mPrestin(N7T,
200 N308S)–transfected cells (Fig. 1c, right), we hypothesised that a short pulse of FUS
201 induced sustained oscillation of Venus-mPrestin(N7T, N308S)–positive puncta that then
202 trigger the calcium response for a few seconds. To address this hypothesis, we found that
203 cellular expression of Venus-mPrestin(N7T, N308S, V499G, Y501H), which prevents the
204 electromotility of prestin without affecting its localisation to the plasma membrane³²,
205 blocked oscillation of the puncta upon FUS stimulation (Fig. 3d, e; Extended Data Video
206 2). Moreover, the lack of oscillation found for the Venus-mPrestin(N7T, N308S, V499G,
207 Y501H) puncta significantly attenuated the FUS-mediated calcium response ($p=0.016$;

208 Fig. 3c). Thus FUS-evoked calcium responses are highly dependent on the electromotility
209 and oscillation of prestin puncta in the plasma membrane.

210 We next determined in which cellular compartment the calcium is stored that is
211 released by Venus-mPrestin(N7T, N308S) upon FUS stimulation. Addition of the calcium
212 chelator ethylene glycol tetraacetic acid (EGTA) in the extracellular space completely
213 inhibited the calcium response in cells expressing Venus-mPrestin(N7T, N308S) upon
214 ultrasound stimulation ($p = 6.2E-7$; Fig. 3f). However, depletion of the intracellular
215 calcium store by thapsigargin did not significantly affect the ultrasound-mediated
216 calcium response ($p = 0.16$; Fig. 3f). Thus mPrestin(N7T, N308S) induced calcium influx
217 from the extracellular space instead of from the intracellular calcium pool after FUS
218 excitation. We speculate that replacement of Asn with Thr and Ser at positions 7 and 308,
219 respectively, in mPrestin enhanced its localisation to the plasma membrane where its
220 oscillations promoted calcium influx from the extracellular pool.

221 Several mechanosensitive ion channels are activated by high-frequency
222 ultrasound^{20,21}. We incubated gentamicin, a pharmaceutical inhibitor of
223 mechanosensitive ion channels, with cells that expressed Venus-mPrestin(N7T, N308S)³³
224 and found that this treatment did not significantly affect the calcium response upon
225 ultrasound excitation ($p = 0.27$; Fig. 3f). Thus gentamicin-sensitive ion channels were not
226 involved in the mPrestin(N7T, N308S)-mediated calcium response, which is consistent
227 with results from an ultrasound-inducible system driven by piezoelectric nanoparticles³⁴.
228 Ultrasound excites neuronal cells by activating voltage-gated ion channels⁶. To examine
229 the possible involvement of voltage-gated ion channels in our system, cells expressing
230 Venus-mPrestin(N7T, N308S) were incubated with tetrodotoxin (TTX), an inhibitor of

231 voltage-gated ion channels, and then stimulated with 0.5 MHz FUS. However, the
232 percentage of ultrasound-excitability cells transfected with mPrestin(N7T, N308S) was not
233 affected by TTX treatment, indicating that voltage-gated ion channels are not involved in
234 the mPrestin-mediated pathway ($p = 0.80$; Fig. 3f).

235 To take advantage of the great sensitivity of Venus-mPrestin(N7T, N308S) to
236 ultrasound stimulation, we next developed a sonogenetic system that would allow for
237 stimulating neurons (Fig. 4). Infection of primary cultured cortical neurons with a Venus-
238 mPrestin(N7T, N308S)-containing lentivirus led to the expression of Venus-
239 mPrestin(N7T, N308S) on a neuronal membrane. Moreover, Venus-mPrestin(N7T,
240 N308S) also forms puncta on neuronal membrane (Fig. 4a). For the sonogenetic
241 stimulation of target neurons in deep brain, an adeno-associated virus (AAV) encoding
242 Venus-mPrestin(N7T, N308S) or Venus alone was injected into the VTA brain region.
243 Two weeks later, anesthetized mice were exposed to transcranial pulsed ultrasonic
244 excitation (0.5 MHz FUS, 0.5 MPa, 5 seconds; Fig. 4b). FUS-activated neurons were
245 mapped by imaging the expression of c-Fos (Fig. 4c). Neuronal excitation was triggered
246 by a short pulsed FUS in Venus-mPrestin(N7T, N308S)-transfected mice ($p = 8.64E-3$,
247 Fig. 4c,d). Control mice with Venus alone expression showed no significant c-Fos
248 expression in VTA region ($p = 0.08$, Fig. 4c,d). These results demonstrated that
249 mPrestin(N7T, N308S)-mediated sonogenetics is a flexible and non-invasive approach
250 for sonogenetic control of neuronal activity.

251 In summary, we here have introduced two evolutionarily conserved amino acid
252 substitutions N7T and N308S into mouse prestin which enhances its self-association as
253 well as puncta formation in the plasma membrane. These mPrestin(N7T, N308S) puncta

254 highly associate with actin filaments and microtubules in cells. A short pulse of 0.5 MHz
255 FUS induces sustained oscillation of mPrestin(N7T, N308S) puncta with electromotility
256 and evokes several waves of calcium responses in transfected cells (Extended Data Fig.
257 4). The ultrahigh ultrasound sensitivity of mPrestin(N7T, N308S) allows for non-
258 invasively stimulation of target neurons in deep mice brain by a short pulsed FUS.

259 Our results raised a fundamental question: why are mPrestin(N7T, N308S)-
260 transfected cells sensitive only to ultrasound of 0.5 MHz? Because we used a short, low-
261 frequency, and low-pressure ultrasound pulse of constant acoustic power (0.5 MPa), it is
262 unlikely that any unexpected thermal and/or mechanical effects were present that would
263 restrict the frequency to 0.5 MHz. We therefore assume that a frequency of 0.5 MHz is
264 simply optimal for stimulation of cells. Cell membranes are able to absorb ultrasound
265 waves and transient cavitation effect occurs in their intramembrane spaces upon
266 ultrasound stimulation³⁵. According to simulation and experimental data, 0.25~0.5 MHz
267 are the optimal frequencies of ultrasound for inducing intramembrane cavitation as well
268 as bio-piezoelectric perturbation^{7,36}. Because prestin acts as a piezoelectric amplifier to
269 enhance the electromotile response in OHCs and mammalian cell lines^{25,26}, we suggest
270 that the ultrasound-induced intramembrane bio-piezoelectric perturbation may be
271 amplified by mPrestin(N7T, N308S) that then trigger the observed calcium influx.
272 Ultrasound of 80 kHz, which is the peak frequency used by most sonar species²³, did not
273 efficiently induce a calcium response in Venus-mPrestin(N7T, N308S)–transfected cells
274 (Fig. 2), which suggested that the mechanism(s) of how sonar-responsive species hear
275 ultrasound by auditory organs may not be the same as in our system.

276 Similar to photon-responsive-proteins and fluorescent proteins, which absorb

277 distinct wavelengths of light and allow for multiplex imaging and optogenetics,
278 mPrestin(N7T, N308S) specifically responds to 0.5 MHz FUS, suggesting that a multiple-
279 frequency system using ultrasound of 1–15 MHz can be developed to non-invasively
280 diagnose regions of abnormal tissues and simultaneously manipulate cellular activities
281 with 0.5 MHz FUS. Moreover, because 0.5 MHz FUS waves cannot be delivered through
282 the air and are rarely used by sonar species, the natural background level for this
283 frequency is expected to be low. Previously developed simulations and experimental data
284 suggest that ultrasound wavelengths of $\sim 0.60\text{--}0.70$ MHz would be optimal for
285 transcranial transmission and brain absorption^{37,38}, supporting that our sonogenetic
286 system is a promising tool for therapeutic applications involving the brain. Indeed, our *in*
287 *vivo* results showed that 0.5 MHz FUS efficiently accesses to the deep brain regions like
288 VTA and stimulates target neurons expressing Venus-mPrestin(N7T, N308S) (Fig. 4c,d).

289 To our knowledge, this mPrestin(N7T, N308S)-based sonogenetic approach is the
290 first system that enables the use of low-frequency ultrasound to efficiently manipulate
291 molecular activities in mammalian cells that are genetically modified. Although
292 heterogeneous expression of mPrestin(N7T, N308S) significantly enhanced the
293 ultrasound sensitivity of HEK293T cells ($p = 0.0046$, $10.18 \pm 2.90\%$ for the Venus-
294 mPrestin(N7T, N308S) group; $1.33 \pm 0.42\%$ for the Venus-alone group; combined data
295 shown in Figs. 1d and 2f), the percentage of ultrasound-excitable cells in our system
296 needs improvement. A more detailed understanding of how mPrestin(N7T, N308S) sense
297 and amplify ultrasound waves is needed to engineer different prestin variants that are
298 more sensitive to ultrasound. With ongoing development, engineered ultrasound-
299 responsive proteins and sonogenetic systems should become versatile and powerful

300 tools for non-invasively and precisely manipulating activities of genetically modified cells.

301

302 **Online Methods**

303 **Cell culture, chemical reagents, DNA constructs, and transfection**

304 Human HEK293T cells were cultured in Dulbecco's modified Eagle's medium (DMEM;
305 Gibco) supplemented with 10% (v/v) fetal bovine serum, 5 U/ml penicillin, and 50 µg/ml
306 streptomycin (Gibco). The following Venus- or CFP-tagged mPrestin mutant genes were
307 generated by site-directed mutagenesis: N7T, N308S, Y667Q, V449G, and Y501H. To
308 construct the pLenti-hSyn1-Venus and pLenti-hSyn1-Venus-mPrestin(N7T, N308S), Q5®
309 High-Fidelity DNA polymerase (New England Biolabs) and HiFi® assembly kit (New England
310 Biolabs) were used. The hSyn1-Venus and hSyn1-Venus-mPrestin(N7T, N308S) inserts were
311 PCR amplified from hSyn1-Venus-mPrestin(N7T, N308S) construct. The pLenti-backbone and
312 the insert with a molar ratio of 1:2 (backbone:fragment) were HiFi® assembled to acquire the
313 corresponding lentiviral vectors. For DNA transfection, LT-1 (Mirus) was used according to
314 the manufacturer's protocol. For inhibitor experiments, gentamicin (200 µM, 20 min, Sigma),
315 TTX (500 nM, 20 min, Abcam), EGTA (5 mM, 20 min, Sigma), and thapsigargin (100 nM,
316 30min, Sigma) were used. Before ultrasound excitation, HEK 293T cells were incubated with
317 one of the various inhibitors or 0.1% (v/v) DMSO dissolved in DMEM (Gibco) at 37°C.
318 Calcium-free, serum-free medium (Gibco) was used in the EGTA experiment.

319

320 **Live-cell imaging**

321 Transfected cells were seeded into a Lab-Tek eight-well chambers (Thermo Scientific)
322 coated with poly-D-lysine (P6407, Sigma-Aldrich) or onto 25-mm cover glasses in six-well

323 culture plates (SPL Life Science) that were similarly coated. Live-cell imaging was conducted
324 using a Nikon T1 inverted fluorescence microscope (Nikon) with a 20× or 60× oil objective
325 (Nikon), a DS-Qi2 CMOS camera (Nikon), and Nikon element AR software (Nikon). The
326 cells were held under a 5% CO₂ atmosphere at 37°C in an environmental chamber (Live Cell
327 Instrument). The distribution of Venus-mPrestin^{WT}, Venus-mPrestin(N7T, N308S),
328 Venus-mPrestin(N7T, N308S, Y667Q), and Venus-mPrestin(N7T, N308S, V499G, Y501H)
329 in HEK293T cells was observed using a Nikon A1 confocal system with a 100× oil
330 objective (Nikon). Multiple *z*-stack images (0.3 μm between stacks; 15 stacks) were
331 acquired and processed with Huygens deconvolution (Scientific Volume Imaging), and
332 the maximum intensity projections of the images were generated by Nikon element AR
333 software. The plasma membrane/cytosol intensity ratios of the Venus-mPrestin
334 constructs were analysed by Nikon element AR software. Ultrafast imaging was acquired
335 under a Nikon A1 confocal system with a Resonant scanner (Nikon) and 100× objective
336 (Nikon).

337

338 **Immunofluorescence staining**

339 HEK293T cells transfected with Venus-mPrestin(N7T, N308S) were seeded on poly-D-
340 lysine-coated Lab-Tek eight-well chambers (Thermo Scientific). Transfected cells were fixed
341 with 4% paraformaldehyde (Electron Microscopy Sciences) at room temperature for 15 min
342 and subsequently permeabilized by 0.1% Triton X-100 (Sigma-Aldrich). After incubation of
343 blocking solution (PBS with 2% bovine serum albumin) for 30 min at room temperature, cells
344 were stained with phalloidin Alexa Fluor 594 (1:100 dilution; Thermo Scientific, A12381) or
345 anti- α -tubulin antibody (1:1000 dilution; Sigma-Aldrich, T6199) for 1 h at room temperature.

346 Goat anti-mouse IgG Alexa Fluor 594 (1:1000 dilution; Thermo Scientific, R37121) were
347 incubated with cells for 1 h at room temperature.

348

349 ***In vitro* FUS stimulation**

350 FUS stimulation (acoustic power, 0.5 MPa; 2000 cycles; pulse repetition frequency, 10
351 Hz; and 3-sec duration) was applied using a single-element FUS transducer (Panametrics). The
352 ultrasound transducer was driven by a function generator (AFG3251, Tektronix) and a radio-
353 frequency power amplifier (80 kHz FUS: 150A100B, AR; 0.5 MHz, 1 MHz, 2 MHz, 3.5 MHz
354 FUS: 325LA, Electronics & Innovation)) to transmit the ultrasound pulses. A water cone filled
355 with degassed water was attached to the ultrasound transducer assembly, after which the
356 surface of the cone was submerged into the culture-dish medium. To record the calcium influx
357 in a cell in real time, the ultrasound transducer was confocally positioned with the objective of
358 the microscope. The transducer was calibrated in the free field in degassed water using a
359 calibrated ultrasound power meter (Model UPM-DP-1AV, Ohmic Instruments Inc.).

360

361 **Lentivirus Production**

362 5 h prior to transfection, culture medium of HEK293T cells grown to a confluency of 60% was
363 replaced with 10 ml DMEM supplemented with GlutaMAX (Gibco, Taipei, Taiwan) and 10%
364 FBS (Hyclone, Taipei, Taiwan) containing 25 μ M chloroquine diphosphate (Tokyo Chemical
365 Industry, Taipei, Taiwan). HEK293T cells were co-transfected with 1.3 pmol psPAX2 (gift
366 from Didier Trono; Addgene plasmid # 12260), 0.72 pmol pMD2.G (gift from Didier Trono;
367 Addgene plasmid # 12259), and 1.64 pmol transfer plasmids (pLenti-hSyn1-Venus or pLenti-
368 hSyn1-Venus-mPrestin(N7T, N308S)) by PEI (Alfa Aesar; 1 mg/ml polyethylenimine, linear,

369 MW25,000) transfection. The ratio of DNA:PEI was 1:3 diluted in 1 ml of OptiMEM (Gibco).
370 18 h post-transfection, viral medium was replaced with 15 ml DMEM supplemented with
371 GlutaMAX and 10% FBS. 48 h post-transfection, viral medium was harvested, stored at 4°C
372 and replaced with 15 ml DMEM supplemented with GlutaMAX and 10% FBS. 72 h post-
373 transfection, viral medium was pooled with the 48 h harvest, and centrifuged at 500 x g for 10
374 min at 4°C. The viral supernatant was filtered through 0.45 µm PES filter (Pall, Taipei, Taiwan),
375 snap frozen with liquid nitrogen, and stored at -80°C.

376

377 **Primary neuronal culture and lentivirus transduction**

378 Sprague-Dawley rats were purchased from BioLASCO Taiwan Co., Ltd. Primary cortical
379 neurons were dissociated from dissected cortices of rat embryos (embryonic day 18, E18) and
380 then seeded on poly-L-lysine (Sigma, Saint Louis, MO) -coated bottom-glass dishes (1.2 x 10⁶
381 cells per dish). On day *in vitro* 0 (DIV0), primary neurons were cultured in Minimum Essential
382 Medium (Invitrogen, Carlsbad, CA) supplemented with 5% fetal bovine serum (Invitrogen),
383 5% horse serum (Invitrogen), and 0.5 mg/ml penicillin-streptomycin (Invitrogen) under 5%
384 CO₂ condition. Culture medium was changed to Neurobasal[®] medium (Gibco, Grand Island,
385 NY) containing 25 µM glutamate (Sigma), 2% B-27[™] supplement (Invitrogen), 0.5 mM L-
386 Glutamine (Invitrogen), and 50 units/ml Antibiotic-Antimycotic (AA) (Invitrogen) on DIV1.
387 10 µM Cytosine-β-D-arabino-furanoside (AraC) (Invitrogen) was added to neurons on DIV2 to
388 inhibit proliferation of glial cells. On DIV3, medium was changed to Neurobasal[®] medium
389 containing 2% B-27[™] supplement, 0.5 mM L-Glutamine and 50 units/ml AA. On DIV6,
390 conditional medium was harvested and half-replaced with fresh Neurobasal/ Glutamine culture
391 medium. Neurons were infected with hSyn1-Venus or hSyn1-Venus-mPrestin(N7T, N308S)-

392 containing lentivirus on DIV7. After overnight incubation at 37°C, the virus-containing
393 medium was replaced with conditional culture medium mixed with equal volume of fresh
394 medium. For further maintenance, the medium was half-changed with fresh Neurobasal/
395 Glutamine culture medium every 2 days. After lentivirus infection for 7 days, neurons were
396 imaged by a Nikon T1 inverted fluorescence microscope (Nikon).

397

398 **Adeno associated virus Viral Delivery**

399 The Venus-mPrestin(N7T, N308S) or Venus alone-containing adeno-associated virus
400 (AAV) were packaged by NTU CVT-LS-AAV core. A total of 1 μ L of AAV encoding Venus-
401 mPrestin(N7T, N308S) or Venus alone were transcranial injected into the left ventral tegmental
402 area (VTA; bregma: - 3 mm, left: 0.5 mm, depth: 4.2 mm). During the experiment, the animal
403 was anesthetized with 2% isoflurane gas and immobilized on a stereotactic frame. After AAV
404 injection for 2 weeks, the mice were simulated by FUS.

405

406 ***In vivo* sonogenetic stimulation of VTA**

407 The AAV transfected mice were randomly divided into four groups: (1) AAV encoding
408 Venus-mPrestin(N7T, N308S) + 0.5 MHz FUS stimulation group; (2) AAV encoding Venus-
409 mPrestin(N7T, N308S) without FUS group(n=3); (3) AAV encoding Venus alone + 0.5 MHz
410 FUS stimulation group (n=3); and (4) AAV encoding Venus alone without ultrasound
411 group(n=3). The 0.5 MHz sonication was applied transcranially at the left brain with the
412 acoustic pressure of 0.5 MPa, 2,000 cycles, and 10 Hz of pulse repetition frequency, sonication
413 duration of 5 sec and one sonication sites. During the experiment, the animal was anesthetized
414 with 2% isoflurane gas and immobilized on a stereotactic frame.

415

416 **Immunohistochemistry staining (IHC)**

417 The successful stimulation of mPrestin(N7T, N308S)-transfected cells was verified by c-
418 Fos IHC staining.³⁹ The brains of mice were removed were sacrificed at 90 min after 0.5 MHz
419 FUS stimulation. The brains were then sliced into 15- μ m sections and incubated into 5% goat
420 serum and PBS for 1 h to block the endogenous proteins. The sections were then incubated in
421 primary rabbit anti-c-Fos antibody (1:1000; SYSY) in antibody diluent for overnight. The
422 sections were then incubated for 1 h in Dylight 594 conjugated anti-rabbit secondary antibody
423 (1:500; GeneTex) in antibody diluent followed by several washes in PBS. The cellular nuclei
424 were labelled by DAPI. Finally, the slides were coverslipped with fluorescent mounting
425 medium and stored flat in the dark at -20°C. The successful transfection of pPrestin was
426 confirmed by the expression of Venus fluorescence protein.

427 We analyzed the overlap between Venus tagged proteins (Venus alone or Venus-
428 mPrestin(N7T, N308S) and c-Fos by calculating the number of Venus positive cells and
429 Venus/c-Fos double positive cells in different animal groups. Means and s.e.m. were calculated
430 across animals, and all statistics were done across animals.

431

432 **Acknowledgments**

433 We thank Dr. Jian Zuo (St. Jude Children's Research Hospital) for the Venus-mouse
434 PrestinWT construct; Dr. Insuk So (Seoul National University College of Medicine) for
435 hTRPC4 α -CFP and mTRPC4 β -CFP constructs; and Dr. Takanari Inoue (Johns Hopkins
436 University School of Medicine) for the CFP-R-GECO, R-GECO, mCherry-CAAX, and
437 mCherry-Giantin constructs. Dr. Takananri Inoue (Johns Hopkins University School of

438 Medicine), Dr. Tsung-Han Kuo (National Tsing Hua University), Dr. Hau-Jie Yau (National
439 Taiwan University) for critical reading of the manuscript. This study was supported in part by
440 the Ministry of Science and Technology (MOST), Taiwan (MOST grant numbers 105-2221-
441 E-007-055 and 105-2119-M-182-001 to C.K.Y. 104-2320-B-007-005-MY2, and 106-2320-B-
442 007-004-MY3 to C.P.L. 104-2311-B-007-001, 105-2628-B-007-001-MY3, 107-2628-B-007-
443 001, and 108-2636-B-007-003 to Y.C.L.). Additional funding consisted of a grant from the
444 Program for Translational Innovation of Biopharmaceutical Development-Technology
445 Supporting Platform Axis (grant number 107-0210-01-19-04) to Y.C.L., start-up funding from
446 the National Tsing Hua University to Y.C.L., a grant from Academia Sinica Innovative
447 Materials and Analysis Technology Exploration (i-MATE) Program (grant number AS-
448 iMATE-107-33) to C.P.L., and a grant from National Health Research Institutes (grant number
449 NHRI-EX108-10813NI) to L.C.

450

451 **Author Contributions**

452 Y.S.H., C.H.F., and N.H. contributed equally to this work. Y.S.H., C.H.F., C.K.Y., and Yu-Chun
453 Lin designed the experiments. C.H.F. and C.Y.W. programmed the ultrasound system, under
454 the supervision of C.K.Y., Y.C.Chang, S.R.H., Y.C.L., W.C.H., and C.Y.C. performed the cell
455 biology experiments. Y.S.H., C.H.F., N.H., Y.C.Chang, Y.C.Chiang, and W.C.H. quantified the
456 imaging results. Y.S.H., S.R.H., Yen-Cheng Lin, and Yu-Chun Lin generated the DNA
457 constructs. A.Y.W. designed and cloned the lentiviral plasmid, V.G. packaged the lentiviruses,
458 C.P.L. supervised the molecular cloning and lentiviral production processes. C.Y.C. prepared
459 the primary cultured cortical neurons under the supervision of L.C. C.H.F. performed the
460 animal experiments. Y.S.H., C.H.F., C.K.Y., and Yu-Chun Lin wrote the paper.

461

462 **Competing interests**

463 The patents of mPresin(N7T, N308S) and relative sonogenetic tools are pending.

464

465 **Supplementary information**

466 Supplementary Information is available in the online version of the paper.

467

468 **References**

- 469 1. Yizhar, O., Fenno, L. E., Davidson, T. J., Mogri, M. & Deisseroth, K. Optogenetics in
470 Neural Systems. *Neuron* **71**, 9–34 (2011).
- 471 2. Sternson, S. M. & Roth, B. L. Chemogenetic Tools to Interrogate Brain Functions.
472 *Annu. Rev. Neurosci.* 387–407 (2014). doi:10.1146/annurev-neuro-071013-014048
- 473 3. Qin, S. *et al.* A magnetic protein biocompass. *Nat. Mater.* **15**, 217–226 (2015).
- 474 4. Stanley, S. A., Sauer, J., Kane, R. S., Dordick, J. S. & Friedman, J. M. Remote
475 regulation of glucose homeostasis in mice using genetically encoded nanoparticles.
476 *Nat. Med.* **21**, 92–98 (2015).
- 477 5. Maresca, D. *et al.* Biomolecular Ultrasound and Sonogenetics. *Annu. Rev. Chem.*
478 *Biomol. Eng.* **9**, annurev-chembioeng-060817-084034 (2018).
- 479 6. Tyler, W. J. *et al.* Remote excitation of neuronal circuits using low-intensity, low-
480 frequency ultrasound. *PLoS One* **3**, (2008).
- 481 7. King, R. L., Brown, J. R., Newsome, W. T. & Pauly, K. B. Effective parameters for
482 ultrasound-induced in vivo neurostimulation. *Ultrasound Med. Biol.* **39**, 312–331
483 (2013).

- 484 8. Tufail, Y. *et al.* Transcranial Pulsed Ultrasound Stimulates Intact Brain Circuits.
485 *Neuron* **66**, 681–694 (2010).
- 486 9. Tufail, Y., Yoshihiro, A., Pati, S., Li, M. M. & Tyler, W. J. Ultrasonic
487 neuromodulation by brain stimulation with transcranial ultrasound. *Nat. Protoc.* **6**,
488 1453–1470 (2011).
- 489 10. Yoo, S. S. *et al.* Focused ultrasound modulates region-specific brain activity.
490 *Neuroimage* **56**, 1267–1275 (2011).
- 491 11. Menz, M. D., Oralkan, O., Khuri-Yakub, P. T. & Baccus, S. a. Precise neural
492 stimulation in the retina using focused ultrasound. *J. Neurosci.* **33**, 4550–4560 (2013).
- 493 12. Tsui, P. H., Wang, S. H. & Huang, C. C. In vitro effects of ultrasound with different
494 energies on the conduction properties of neural tissue. *Ultrasonics* **43**, 560–565 (2005).
- 495 13. Foley, J. L. J., Little, J. W. J. J. W. & Vaezy, S. Image-guided high-intensity focused
496 ultrasound for conduction block of peripheral nerves. *Ann. Biomed. Eng.* **35**, 109–119
497 (2007).
- 498 14. Meijering, B. D. M. *et al.* Ultrasound and microbubble-targeted delivery of
499 macromolecules is regulated by induction of endocytosis and pore formation. *Circ.*
500 *Res.* **104**, 679–687 (2009).
- 501 15. Fan, Z., Liu, H., Mayer, M. & Deng, C. X. Spatiotemporally controlled single cell
502 sonoporation. *Proc. Natl. Acad. Sci.* **109**, 16486–16491 (2012).
- 503 16. Ibsen, S., Tong, A., Schutt, C., Esener, S. & Chalasani, S. H. Sonogenetics is a non-
504 invasive approach to activating neurons in *Caenorhabditis elegans*. *Nat. Commun.* **6**,
505 1–12 (2015).
- 506 17. Dynamic, W. B. *et al.* Targeted Microbubbles for Imaging Tumor Angiogenesis :

- 507 Assessment of Purpose : Methods : Results : Conclusion : **249**, (2008).
- 508 18. Lakshmanan, A. *et al.* Molecular Engineering of Acoustic Protein Nanostructures. *ACS*
509 *Nano* **10**, 7314–7322 (2016).
- 510 19. Bourdeau, R. *et al.* Acoustic reporter genes for non-invasive imaging of microbes in
511 mammalian hosts. *Nat. Publ. Gr.* **553**, 86–90 (2018).
- 512 20. Prieto, M. L., Firouzi, K., Khuri-Yakub, B. T. & Maduke, M. Activation of Piezo1 but
513 Not NaV1.2 Channels by Ultrasound at 43 MHz. *Ultrasound Med. Biol.* **44**, 1217–
514 1232 (2018).
- 515 21. Ye, J. *et al.* [ASAP] Ultrasonic Control of Neural Activity through Activation of the
516 Mechanosensitive Channel MscL. *Nano Lett.* (2018).
517 doi:10.1021/acs.nanolett.8b00935
- 518 22. Fettiplace, R. & Hackney, C. M. The sensory and motor roles of auditory hair cells.
519 *Nat. Rev. Neurosci.* **7**, 19–29 (2006).
- 520 23. Rossiter, S. J., Zhang, S. & Liu, Y. Prestin and high frequency hearing in mammals.
521 *Commun. Integr. Biol.* (2011). doi:10.4161/cib.4.2.14647
- 522 24. Liu, Z., Qi, F.-Y., Zhou, X., Ren, H.-Q. & Shi, P. Parallel Sites Implicate Functional
523 Convergence of the Hearing Gene Prestin among Echolocating Mammals. *Mol. Biol.*
524 *Evol.* **31**, 2415–2424 (2014).
- 525 25. Dallos, P. & Fakler, B. Prestin, a new type of motor protein. *Nat. Rev. Mol. Cell Biol.*
526 **3**, 104–111 (2002).
- 527 26. Ludwig, J. *et al.* Reciprocal electromechanical properties of rat prestin: the motor
528 molecule from rat outer hair cells. *Proc. Natl. Acad. Sci. U. S. A.* **98**, 4178–4183
529 (2001).

- 530 27. Song, H. B., Jun, H. O., Kim, J. H., Fruttiger, M. & Kim, J. H. Suppression of transient
531 receptor potential canonical channel 4 inhibits vascular endothelial growth factor-
532 induced retinal neovascularization. *Cell Calcium* **57**, 101–108 (2015).
- 533 28. Myeong, J., Kwak, M., Hong, C., Jeon, J. H. & So, I. Identification of a membrane-
534 targeting domain of the transient receptor potential canonical (TRPC)4 channel
535 unrelated to its formation of a tetrameric structure. *J. Biol. Chem.* **289**, 34990–35002
536 (2014).
- 537 29. Zhang, Y., Moeini-Naghani, I., Bai, J., Santos-Sacchi, J. & Navaratnam, D. S.
538 Tyrosine motifs are required for prestin basolateral membrane targeting. *Biol. Open*
539 197–205 (2015). doi:10.1242/bio.201410629
- 540 30. Greeson, J. N., Organ, L. E., Pereira, F. a. & Raphael, R. M. Assessment of prestin
541 self-association using fluorescence resonance energy transfer. *Brain Res.* **1091**, 140–
542 150 (2006).
- 543 31. Mio, K. *et al.* The motor protein prestin is a bullet-shaped molecule with inner cavities.
544 *J. Biol. Chem.* **283**, 1137–1145 (2008).
- 545 32. Zheng, J. *et al.* The C-terminus of prestin influences nonlinear capacitance and plasma
546 membrane targeting. *J. Cell Sci.* **118**, 2987–2996 (2005).
- 547 33. Jacques-Fricke, B. T. Ca²⁺ Influx through Mechanosensitive Channels Inhibits
548 Neurite Outgrowth in Opposition to Other Influx Pathways and Release from
549 Intracellular Stores. *J. Neurosci.* **26**, 5656–5664 (2006).
- 550 34. Marino, A. *et al.* Piezoelectric Nanoparticle-Assisted Wireless Neuronal Stimulation.
551 *ACS Nano* **9**, 7678–7689 (2015).
- 552 35. Krasovitski, B., Frenkel, V., Shoham, S. & Kimmel, E. Intramembrane cavitation as a

- 553 unifying mechanism for ultrasound-induced bioeffects. *Proc. Natl. Acad. Sci.* **108**,
554 3258–3263 (2011).
- 555 36. Plaksin, M., Shoham, S. & Kimmel, E. Intramembrane cavitation as a predictive bio-
556 piezoelectric mechanism for ultrasonic brain stimulation. *Phys. Rev. X* **4**, 1–10 (2014).
- 557 37. White, P. J., Clement, G. T. & Hynynen, K. Local frequency dependence in
558 transcranial ultrasound transmission. *AIP Conf. Proc.* **829**, 256–260 (2006).
- 559 38. Hayner, M. & Hynynen, K. Numerical analysis of ultrasonic transmission and
560 absorption of oblique plane waves through the human skull. *J. Acoust. Soc. Am.* **110**,
561 3319–3330 (2001).

562

563 **Figure legends**

564 **Figure 1 | mPrestin carrying the N7T and N308S mutations functions as an ultrasound-**
565 **responsive protein. (a)** Sequence alignment of prestins from six non-echolocating and eight
566 echolocating species showing that N7T and N308S substitutions frequently occurred in the
567 echolocating species. Positions 7 and 308 are boxed with the residues located at those positions
568 highlighted in red. **(b)** Excitation of 0.5 MHz FUS evokes calcium responses in cells expressing
569 Venus-mPrestin(N7T, N308S) but not in control cells expressing Venus alone. Cells were co-
570 transfected with the calcium biosensor CFP-R-GECO. The intensity of the R-GECO
571 fluorescence in the cells was monitored by live-cell imaging. Scale bar, 10 μ m. **(c)** Time course
572 of R-GECO fluorescence intensity in cells expressing the indicated constructs before and after
573 the 0.5 MHz FUS as described above. ATP treatment (10 μ M) served as a positive control to
574 show that the cells could exhibit intracellular calcium flux. Data were collected for 7–36
575 independent experiments, with $n = 250$ cells per experiment.

576

577 **Figure 2 | mPrestin(N7T, N308S) enabled an ultrasound-evoked calcium response in a**
578 **frequency-specific manner.** HEK293T cells transfected with one of the indicated DNA
579 constructs were bathed in PBS and stimulated with ultrasound of different frequencies (3-sec
580 duration, 2000 cycles, 0.5 MPa). Data are presented as the relative percentage of cells in each
581 group (expressed as fold-probability) that were excitable by ultrasound after normalisation to
582 that of cells expressing only Venus that were stimulated at the same frequency. The absolute
583 number of cells in each group was 998, 556, 686, 739, 780, 3111, 438, 277, 691, 1484, 1515,
584 408, 472, 785, 771, 1735, 856, 1571, 1085, 520, 1470, 1050, 1250, 1199, and 605 cells from
585 left to right. Data are shown as the mean \pm s.e.m. for 7–36 independent experiments. *P*-values
586 > 0.05 are not shown.

587

588 **Figure 3 | mPrestin(N7T, N308S) puncta oscillate upon FUS stimulation and trigger**
589 **calcium influx from extracellular pool. (a)** Representative confocal images of HEK293T
590 cells expressing Venus-mPrestinWT, Venus-mPrestin(N7T, N308S), mCherry-CAAX (a
591 plasma membrane marker), or mCherry-Giantin (a Golgi marker). For each field, the maximum
592 *z*-projection was created from 15 stacks, each separated by 0.3 μm . Scale bar, 10 μm **(b)**
593 Quantification of the plasma membrane/cytosol ratio for the indicated mPrestin constructs.
594 Data are shown as the mean \pm s.e.m. for three independent experiments; *n* = 22, 26, and 61
595 cells from left to right. **(c)** HEK293T cells expressing the indicated constructs were stimulated
596 with 0.5 MHz FUS (3-sec duration, 2000 cycles, 0.5 MPa). Data are presented as in Figure 2.
597 The absolute number of cells in each group was 3111, 438, 1484, 532, and 430 cells from left
598 to right. The data are shown as the mean \pm s.e.m. for 6–36 independent experiments. **(d)** Video

599 frames showing the structural dynamics of mPrestin-positive puncta in cells that had or had not
600 been stimulated with 0.5 MHz FUS. The boundaries of the punctate regions are outlined in
601 white. Scale bar, 0.2 μm . (e) Area measurements of mPrestin-positive puncta with or without
602 FUS stimulation. (f) HEK293T cells expressing Venus-mPrestin(N7T, N308S) were incubated
603 with EGTA (5 mM, 20 min), thapsigargin (100 nM, 30 min), gentamycin (200 μM , 20 min), or
604 TTX (500 nM, 20 min) in DMEM and were stimulated with 0.5 MHz FUS (3-sec duration,
605 2000 cycles, 0.5 MPa); 0.1% DMSO served as the control. Data are presented as in Figure 1b.
606 The absolute number of cells in each group was 1642, 1238, 1826, 1996, 566, and 772 from
607 left to right. Data are shown as the mean \pm s.e.m. for 6–12 independent experiments.

608

609 **Figure 4 | Transcranial FUS stimulation of neuron in mice brain via mPrestin(NT, NS)**
610 **expression.** (a) A representative image of primary cultured cortical neurons expressing Venus-
611 mPrestin(N7T, N308S). The maximum z-projection was created from 15 stacks, each separated
612 by 0.3 μm . Scale bar, 20 μm . (b) In vivo experimental scheme for transcranial FUS stimulation
613 of the VTA in anesthetized mice. (c) Representative images of mice brain sections with
614 different conditions. Extensive FUS-driven c-Fos (red) expression was detected in cells
615 expressing Venus-mPrestin(N7T, N308S) after FUS stimulation. Arrows indicate c-
616 Fos+Venus+ cells. Scale bar, 100 μm . (d) Percentage of c-Fos-positive neurons expressing
617 Venus alone or Venus-mPrestin(N7T, N308S) with or without FUS stimulation. Data are shown
618 as the mean \pm s.e.m. for 6~9 different sections from 4 mice per condition.

619

620 **Extended Data Figure 1 | Our computer-controlled live-cell imaging and ultrasound-**
621 **exposure system.** An ultrasound transducer connected to an amplifier and waveform generator

622 was placed in the medium of a culture dish containing a monolayer of cells for FUS excitation.

623 The behaviour of cells upon FUS stimulation in real time was observed through an inverted
624 microscope.

625

626 **Extended Data Figure 2 | mTRPC4 β enabled a weak ultrasound-evoked calcium response**

627 **in a frequency-specific manner.** HEK293 cells transfected with one of the indicated DNA

628 constructs were bathed in PBS and stimulated with ultrasound of different frequencies (3-sec

629 duration, 2000 cycles, 0.5 MPa). Data are presented as the relative number of cells in each

630 group (expressed as fold-probability) that were excitable by ultrasound after normalisation to

631 that of cells expressing only Venus that were stimulated at the same frequency. The absolute

632 number of cells in each group was 1209, 768, 889, 1634, 1665, 1736, 1054, 1035, 1116, 1012,

633 1000, 960, 1168, 857, and 909 cells from left to right. Data are shown as the mean \pm s.e.m. for

634 7–17 independent experiments. *P* values > 0.05 are not shown.

635

636 **Extended Data Figure 3 | Characterization of mPrestin(N7T, N308S)-positive puncta. (a)**

637 The average number of mPrestin-positive puncta in cells expressing the indicated constructs.

638 The number of cells counted in each group are 7, 3, and 3 cells from 3 independent experiments.

639 Data are shown as mean \pm s.e.m. **(b)** Size distribution of mPrestin(N7T, N308S)-positive

640 puncta. *n* = 101 puncta from five cells expressing mPrestin(N7T, N308S). **(c)** HEK293 cells

641 transfected with the indicated DNA constructs were imaged by fluorescence resonance energy

642 transfer (FRET). Scale bars, 10 μ m. **(d)** Quantification of the FRET/CFP ratios for cells

643 expressing the indicated DNA constructs. The numbers of cells were 25 (mPrestinWT) and 21

644 (mPrestin(N7T, N308S)). Data are shown as the mean \pm s.e.m. for two independent experiments.

645 (e) HEK293T cells expressing Venus-mPrestin(N7T, N308S) were processed for
646 immunofluorescence with phalloidin (actin filaments) or anti- α -tubulin antibody
647 (microtubules). For each field, a maximal z projection was created from 15 stacks separated by
648 0.3 μ m. Scale bar= 10 μ m.

649

650 **Extended Data Figure 4 | The working model of mPrestin(N7T, N308S)-mediated calcium**
651 **influx upon ultrasound stimulation.** Two evolutionarily conserved mutants N7T and N308S
652 enhance self-assembly of mPrestin in the punctate regions of plasma membrane where they
653 associate with actin filaments and microtubules. The mPrestin(N7T, N308S)-positive puncta
654 with electromotility are oscillated upon 0.5 MHz FUS stimulation (3-sec duration, 2000 cycles,
655 0.5 MPa) which triggers the influx of calcium from extracellular space.

656

657 **Extended Data Video 1 | mPrestin(N7T, N308S) enables ultrasound-evoked calcium**
658 **response.** Excitation of 0.5 MHz FUS evokes calcium response in cells expressing Venus-
659 mPrestin(N7T, N308S) but not in control cells (Venus alone). The cells co-transfected with a
660 calcium biosensor, CFP-R-GECO, and Venus alone or Venus-mPrestin(N7T, N308S), were
661 excited by 0.5 MHz pulsed FUS (3 sec duration, 2000 cycles, 0.5 MPa). The intensity of R-
662 GECO in cells was monitored by live-cell imaging. Scale bar = 10 μ m.

663

664 **Extended Data Video 2 | mPrestin(N7T, N308S)-positive puncta oscillated upon FUS**
665 **stimulation.** HEK293T cells were transfected with Venus-mPrestin(N7T, N308S) or Venus-
666 mPrestin(N7T, N308S, V499G, Y501H). Video showing the structural dynamics of mPrestin-
667 positive puncta in cells that had or had not been stimulated with 0.5 MHz FUS. The boundaries

668 of the punctate regions are outlined in white. Scale bar = 0.2 μm .

669

Figure 1

a

Non-echolocating species	<i>Homo sapiens</i>	1MDHAEENE I LAATQRYYYVER20	301 TGI SAGFNLKESYNVDVVG319
	<i>Mus musculus</i>	1MDHAEENE I PAETQRYYYVER20	301 TGI SAGFNLHESYSVDVVG319
	<i>Pteropus vampyrus</i>	1MDHAEENE I LAATQRYYYVER20	301 TGI SAGFNLHESYNVDVVG319
	<i>Balaenoptera acutorostrata</i>	1MDHAEENE I LAAAQRYYYVER20	301 TGI SAGFNLNESYNVDVVG319
	<i>Eonycteris spelaea</i>	1MDHAEENE I LAATQRYYYVER20	301 TGI SAGFNLHESYNVDVVG319
	<i>Rousettus leschenaultia</i>	1MDHAEENE I LAATQRYYYVER20	301 TGI SAGFNLHESYNVDVVG319
	Echolocating species	<i>Phocoena phocoena</i>	1MDHVEESE I LAATQRYYYVER20
<i>Megaderma spasma</i>		1MDHAEETE I LAATQKYYVER20	301 TGI SAGFSLHESYNVDVVG319
<i>Megaderma lyra</i>		1MDHAEETE I LAATQKYYVER20	301 TGI SAGFSLHESYNVDVVG319
<i>Hyperoodon ampullatus</i>		1MDHVEETE I LAATQRYYYVER20	301 TGI SAGFNLHESYNVDVVG319
<i>Ziphius cavirostris</i>		1MDHVEETE I LAATQRYYYVER20	301 TGI SAGFNLHESYNVDVVG319
<i>Miniopterus fuliginosus</i>		1MDHAEETE I LAATQRYCVDR20	301 TGI SAGFSLHESYNVDVVG319
<i>Tursiops truncatus</i>		1MDHVEETE I LAATQRYYYVER20	301 TGI SAGFSLHESYNVDVVG319
	<i>Myotis ricketti</i>	1MDHAEETE I LAAAKYYVDR20	301 TGI SAGFSLHESYNVDVVG319

bioRxiv preprint doi: <https://doi.org/10.1101/625533>; this version posted May 3, 2019. The copyright holder for this preprint (which was not certified by peer review) is the author/funder. All rights reserved. No reuse allowed without permission.

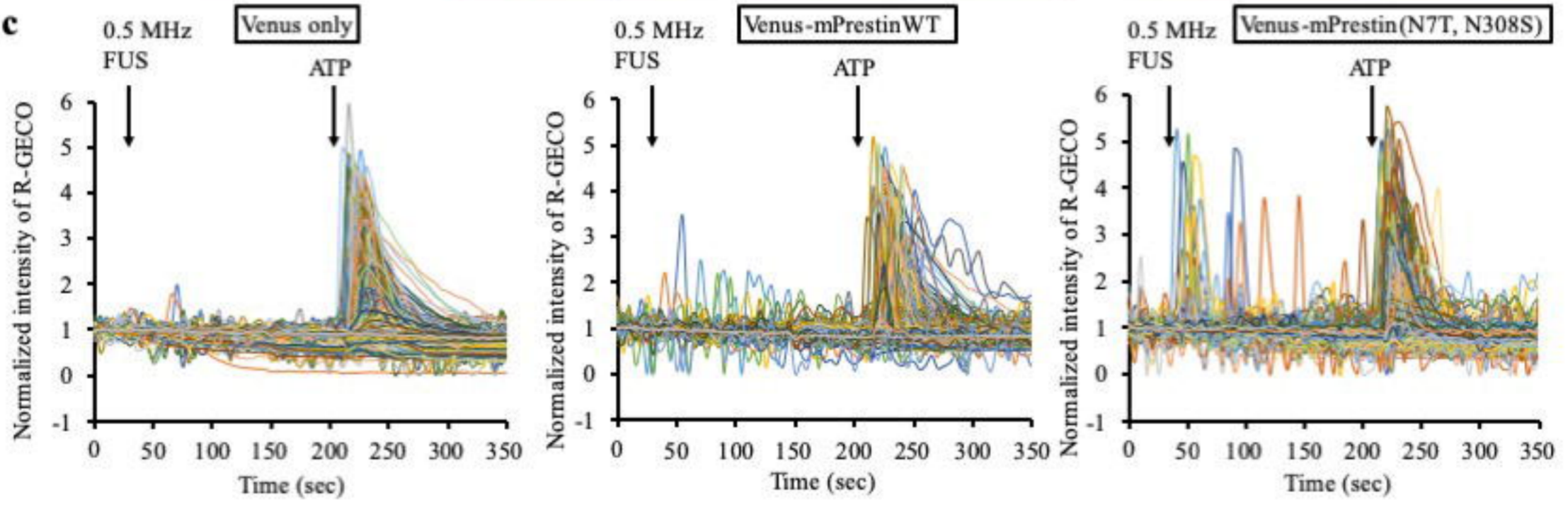
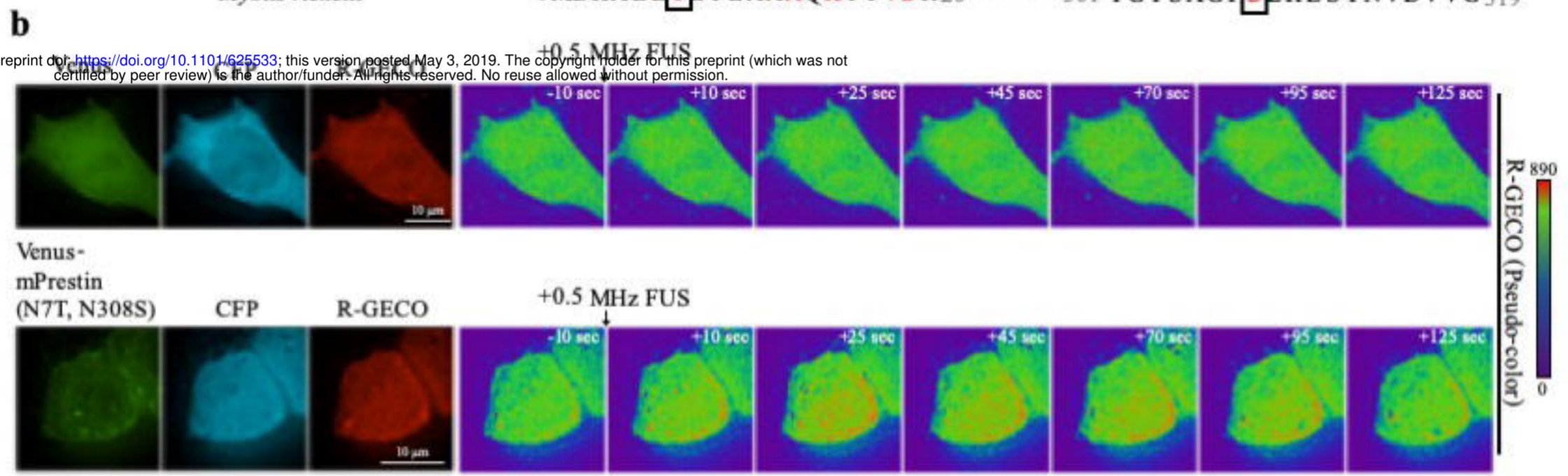


Figure 2

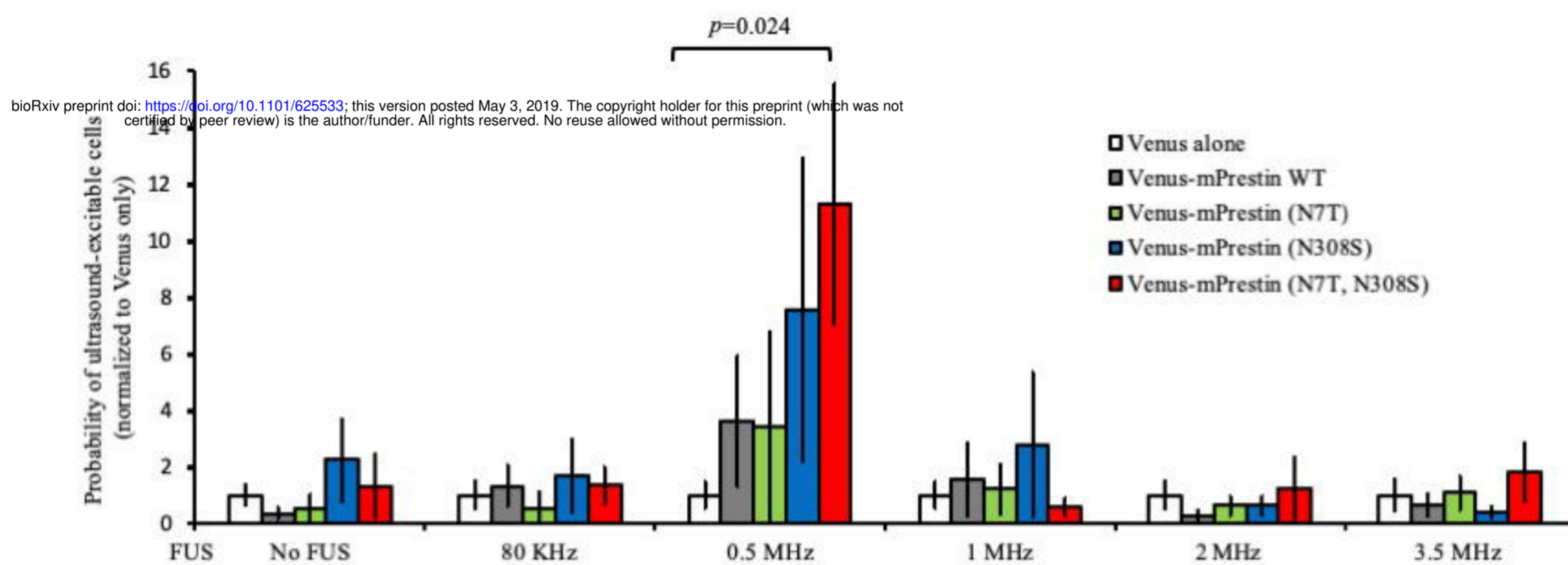


Figure 3

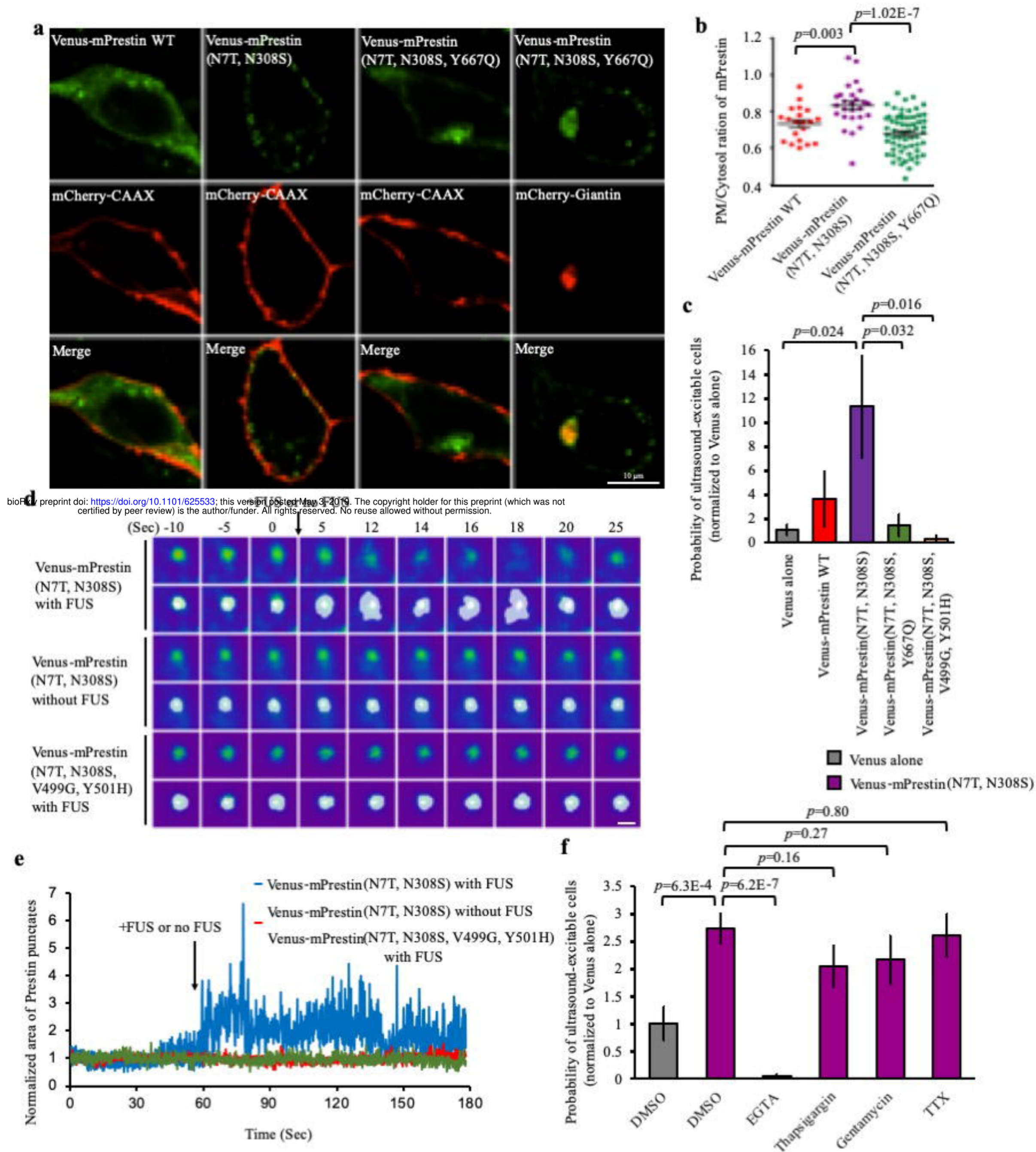
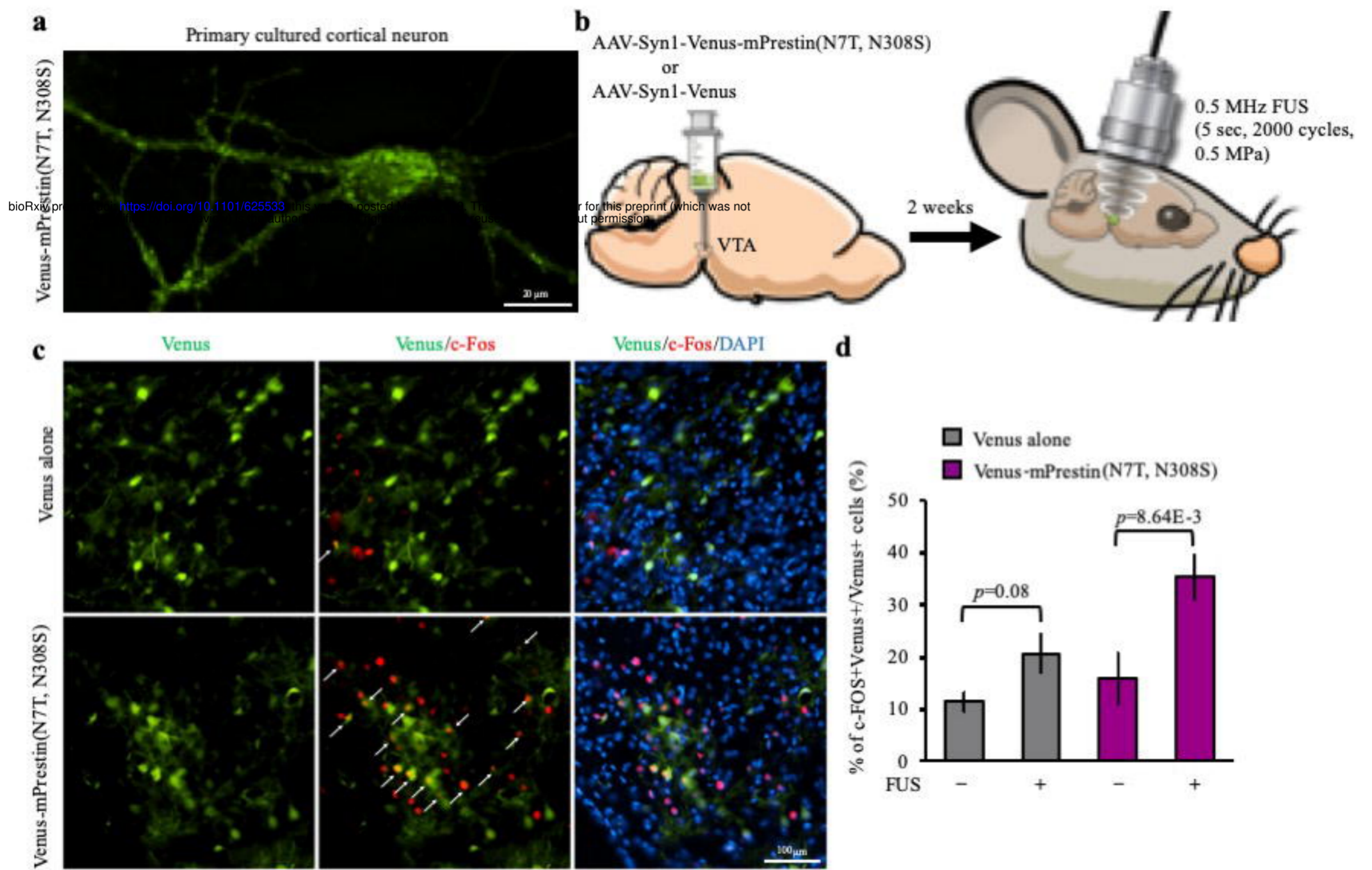
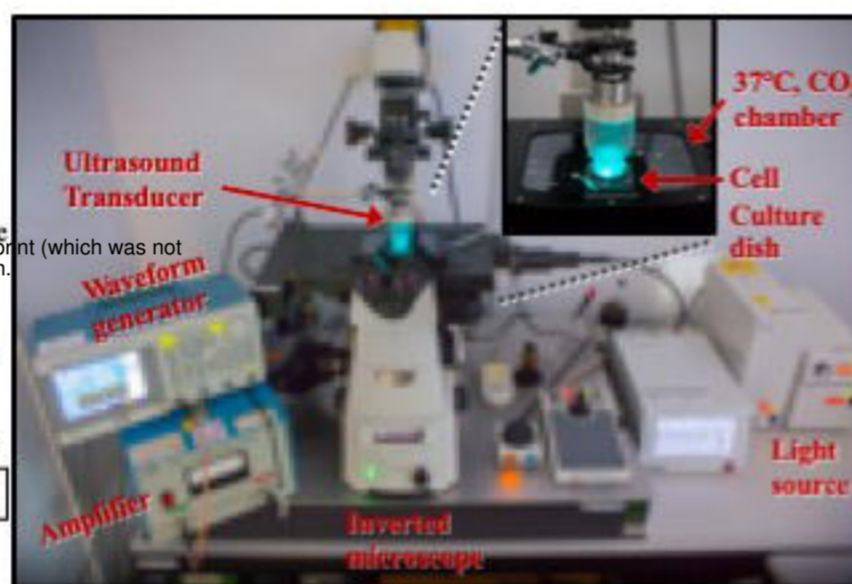
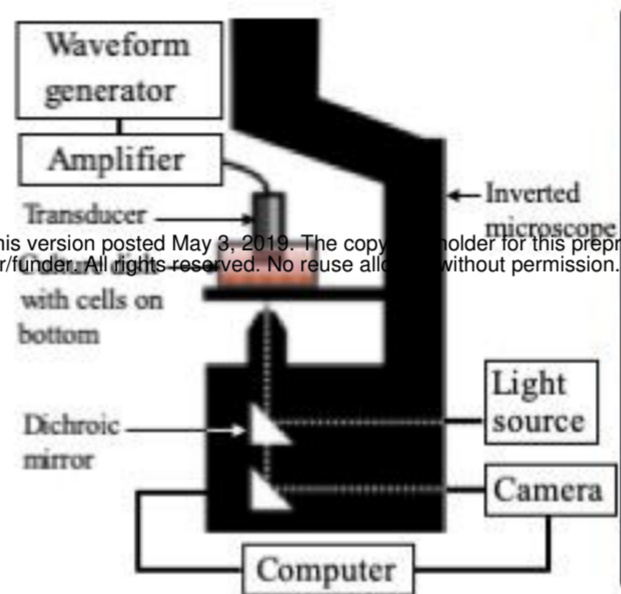


Figure 4

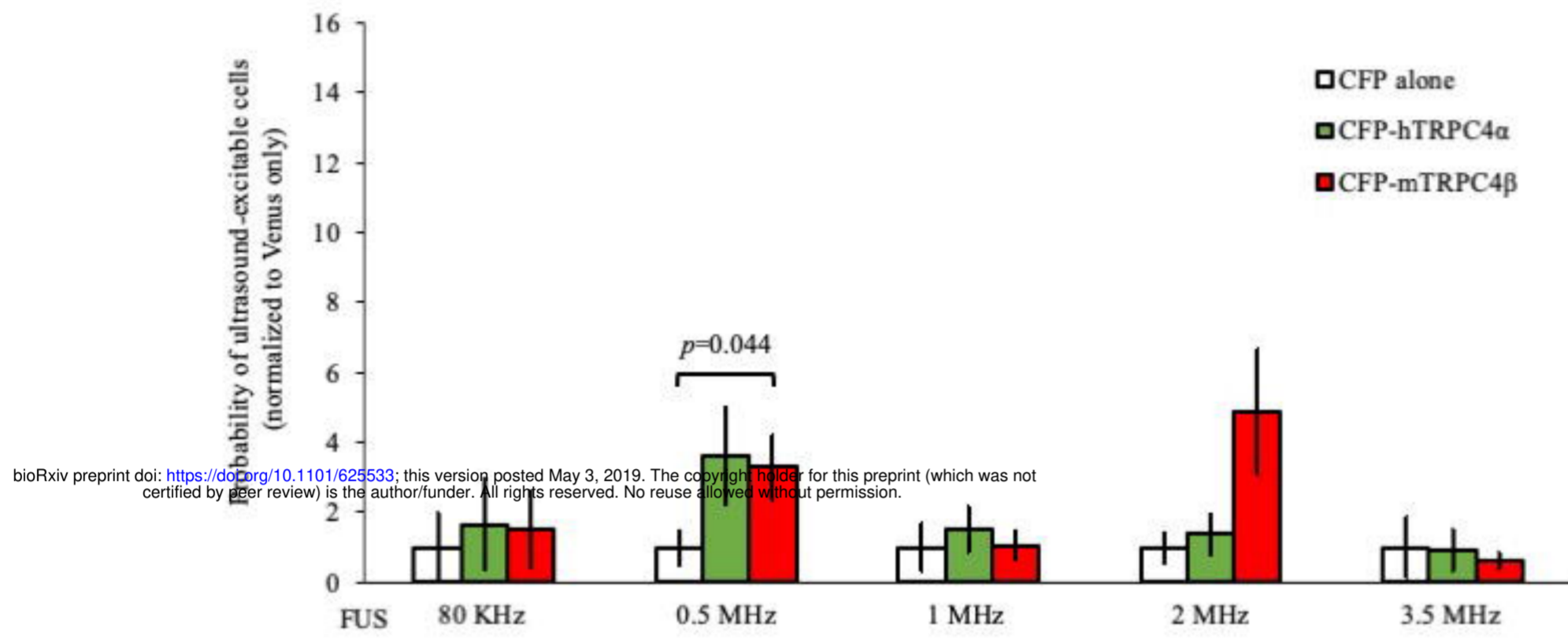


Extended Figure 1

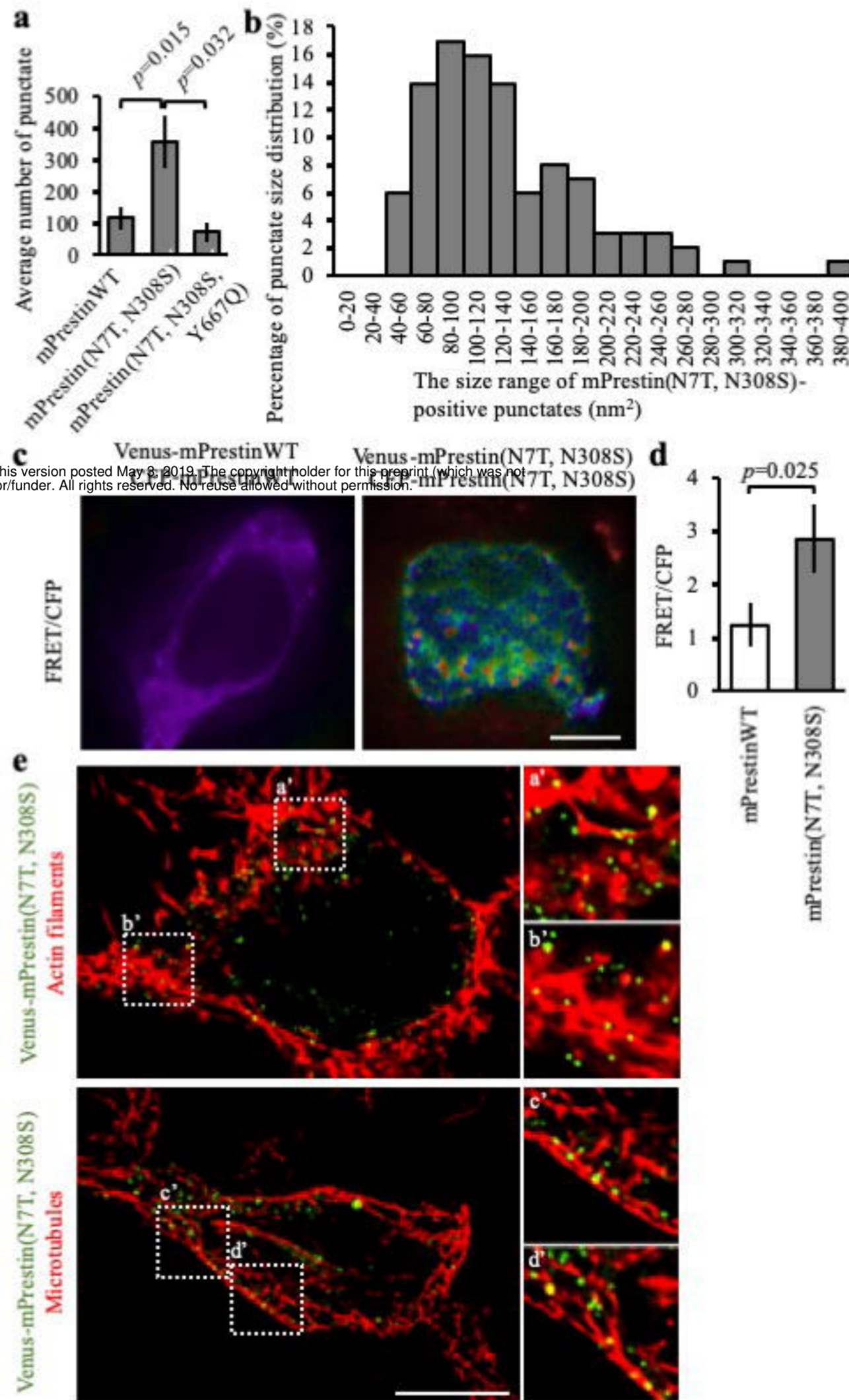
bioRxiv preprint doi: <https://doi.org/10.1101/625533>; this version posted May 3, 2019. The copyright holder for this preprint (which was not certified by peer review) is the author/funder. All rights reserved. No reuse allowed without permission.



Extended Figure 2



Extended Figure 3



bioRxiv preprint doi: <https://doi.org/10.1101/625533>; this version posted May 8, 2019. The copyright holder for this preprint (which was not certified by peer review) is the author/funder. All rights reserved. No reuse allowed without permission.

Extended Figure 4

bioRxiv preprint doi: <https://doi.org/10.1101/625533>; this version posted May 3, 2019. The copyright holder for this preprint (which was not certified by peer review) is the author/funder. All rights reserved. No reuse allowed without permission.

